July 2008 *Volume 4 Issue 4*

Trade Science Inc.

Materials Science

An Indian Journal

Full Paper

MSAIJ, 4(4), 2008 [342-349]

Synthesis of $CoNi_2O_3$ and kinetics of thermal decomposition of the oxalate precursor by constant transformation rate thermal analysis (CRTA) under vacuum

Kais Nahdi*, Malika Trabelsi Ayedi

Laboratoire des Applications de la Chimie aux Ressources et Substances Naturelles et a l'Environnement (LaCReSNE), Faculte des Sciences de Bizerte, 7021, Zarzouna, Bizerte, (TUNISIE)

Tel.: +216 23 98 77 60; Fax: +216 72 590 566

E-mail: k_nahdi@yahoo.fr

Received: 17th June, 2008 ; Accepted: 22nd June, 2008

ABSTRACT

The thermal decomposition processes taking place in the solid state oxalate mixture of $CoC_2O_4.2H_2O$-$NiC_2O_4.2H_2O$ (1:2 mole ratios) in air have been studied using TG-DTG and DSC techniques. The parent mixture and mixtures calcined at different temperatures in air were characterized using XRD and FT-IR techniques. The Kinetic analysis of the thermal decomposition of the binary oxalates mixture was performed by Controlled Rate Thermal Analysis technique under residual partial pressure of 10^{-3}hPa. The activation energy for each decomposition step was measured experimentally and the possible conversion function $f(\alpha)$ was investigated.

KEYWORDS

$CoNi_2O_3$;
XRD;
Kinetic;
Controlled rate thermal analysis;
TG-DTG;
DSC.

1. INTRODUCTION

Investigation of chemical, physical and structural properties of mixed metal oxides have found very important applications in new technologies. They can be used as prospective materials for magnetic recording, many electronic components, sensors, catalysts as well as the high-temperature superconductors.

Cobalt-based perovskite-type oxides are being increasingly applied to electronic and magnetic materials, as well as to automotive exhaust catalysts and electrode materials for fuel cells.

In its reduced form nickel oxide has been mainly used for such reactions as the hydrogenation of nitriles [1-3] and hydrodechlorination of aromatic compounds[4,5]. El waheb et al.[6] reported gamma irradiation effects on the electrical conductivity behaviour and thermal decomposition induction period in nickel oxalate. Poizot et al.[7] found that transition metal oxide, especially NiO and CoO, demonstrate high lithium storage capacity.

The key factor in obtaining oxides with different properties has been the use of different preparative methods. In the literature, we have found nickel and cobalt oxides which have been prepared with thermal decomposition of oxalate precursor. The binary mixture of nickel oxalate and cobalt oxalate has not been investigated as the precursor's nickel-based oxide.

Conventional isothermal and dynamic methods of thermogravimetric technique have been used for studying the kinetics of the thermal decomposition reactions of oxalates. The kinetic of $CoC_2O_4.2H_2O$ dehydration reaction showed that it is controlled by phase boundary reaction (R2-R3) mechanism with activation energy equal to 89kJ.mol^{-1}[8]. Whereas the kinetic of CoC_2O_4 decomposition was showed obeyed the Avrami-Erofeev (A2) mechanism[9]. The corres

ponding activation energy was found depending on the method of data processing and range from 137 to 250kJ.mol^{-1}.

For the kinetic of anhydrous Nickel oxalate decom position, it was found obeying to A2 mechanism when studied by isothermal method[10-13] and to F1[14-15] or A4[16] when studied by rising temperature. The reported activation energies are in the range 121-174kJ.mol^{-1}. No data information was found in the literature about the kinetic of the thermal dehydration of $NiC_2O_4.2H_2O$.

The present work reports a study of the thermal decompositions in air of individual cobalt oxalate crystallohydrate and nickel oxalate crystallohydrate as well as their mixture with mole ratio1:2 via TG-DTG and DSC techniques. The parent mixtures and mixtures calcined at different temperatures were characterized using XRD and FT-IR techniques to give some information about the decomposition pathway.

The kinetics of the thermal dehydration and decomposition of the binary oxalates mixture were also investigated using controlled rate thermal analysis technique under low residual partial pressure of 10^{-3}hPa.

2. EXPERIMENTAL

2.1 Materials

Individual metal oxalates were prepared by precipitation from aqueous solutions containing the calculation amounts of AR metal chloride salt with equimolar quantity of AR oxalic acid. The fine precipitate obtained were filtered, washed with distilled water until free of chloride ions and dried. The oxalate precursor was prepared by physical mixture of $CoC_2O_4.2H_2O$-$NiC_2O_4.2H_2O$ (1:2 mole ratio) using the impregnation technique[17] by thoroughly mixing the desired mole ratio of pure oxalates, then the mixture was dried in a thermostated oven at 50°C for 2h.

2.2. Experimental apparatus

TG-DTG analyses were performed, using a commercial apparatus (TA Instruments, Q500). Samples of the individual and binary oxalates mixture were analyzed at heating rate of 10K.min^{-1} in air flow. The sample mass in the Pt cell of the thermogravimetric analyzer was kept at about 10 mg in all experiments.

The differential scanning calorimetry (DSC) analyses were performed on a Mettler-Toledo DSC822e (Switzerland). Samples were analyzed at a heating rate of 10K.min^{-1} in air.

The sample mass in the aluminous pan (Shanghai Balance Plant, 40 ml) was kept at about 5 mg. The reference pan was pure aluminum pan. The temperature and energy of instrument had been calibrated by standard metal In, before all measures.

The calcination of the oxalates mixture has been carried out in a Programmable Electric Furnace (Nabertherm) at a heating rate of 10K.min^{-1} under air atmosphere.

XRD patterns for the different calcined samples were recorded at room temperature by means of a Bruker X-ray diffraction unit using a Cu target.

Transmission electron microscopy (TEM) analyses were carried out using a TECNAI G^2 equipment to well characterize the synthesized powder. The local chemical composition was determined making use of EDAX.

CRTA experiments were carried out with 200 mg sample weighed into a fused silica cell which is placed into a refrigerated furnace constructed in house and operating in the temperature range from 248K up to 873K. Once the equilibrium temperature is reached, the pressure above the sample, measured by a Pirani gauge, is lowered, using vacuum pumping system from 1 bar to the desired value (10-3 hPa in our case). During the CRTA experiment where the reaction leads to the production of a vapor, the vapor pressure is measured by a Pirani gauge placed in proximity of the sample. The pressure signal produced by the Pirani gauge is sent to the furnace heating controller. The heating of the sample then takes place in such a way that the vapor pressure above the sample (and upstream the evacuation diaphragm) remains constant. A detailed description of the set-up can be found in[18].

3. RESULTS AND DISCUSSION

3.1. TG–DTG analyses

TG-DTG curves for the individual oxalates and the binary mixture are shown in figure 1. The thermal decomposition, in the temperature range up to 973K, of $CoC_2O_4.2H_2O$ and $NiC_2O_4.2H_2O$ proceeds via two well-defined steps. The first step in the thermal decomposition of $CoC_2O_4.2H_2O$ (figure 1a) is a dehydration step, which occurs in the temperature range 400K-473K. The weight loss accompanying this step amounts to about 18.90% in accordance with calculated weight loss of 19.7% attributed to the complete dehydration.

Full Paper

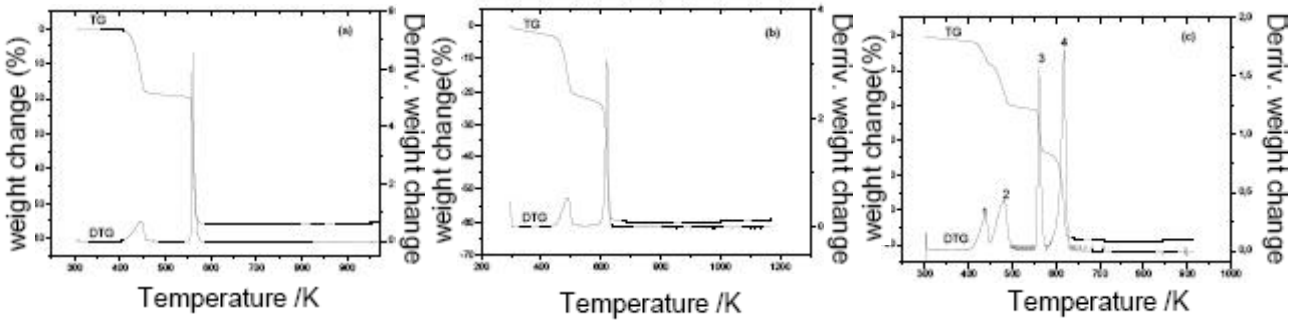

Figure 1: TG-DTG curves of $CoC_2O_4.2H_2O$ (a), $NiC_2O_4.2H_2O$ (b) and of the binary mixture (c)

TABLE 1: The mass loss data and the suggested products for the decomposition of $CoC_2O_4.2H_2O$-$NiC_2O_4.2H_2O$ (1:2 mol ratio) binary mixture at a heating rate of 10K.min^{-1} in air

Thermal step	Temperature range (K)	Mass loss (%) Calculated	Theoretical	Suggested product
1	404-448	7.02	6.56	CoC_2O_4-$NiC_2O_4.2H_2O$
2	448-497	12.61	13.13	CoC_2O_4-NiC_2O_4
3	525-579	12.73	12.16	Co_3O_4-NiC_2O_4
4	579-649	26.01	26.26	Co_3O_4-NiO

The anhydrous cobalt oxalate, decomposed in the second step, indicates a weight loss of 37.27% which is in accordance with calculated weight loss of 36.44% due to the formation of Co_3O_4.

The first step in the thermal decomposition of $NiC_2O_4.2H_2O$ (figure 1b), which occurs in the temperature range 428K-505K, shows a weight loss of 20.42% in agreement with calculated weight loss of 19,77% attributed to the formation of NiC_2O_4. This latter, decomposed in the second step, gives a weight loss of 39.59% which is in accordance with calculated weight loss of 39,41% characteristic for the production of NiO.

Figure 1c displays the TG-DTG curves obtained for $CoC_2O_4.2H_2O$-$NiC_2O_4.2H_2O$ (1:2 mole ratio) binary mixture in air at heating rate of 10K.min^{-1}. From the TG curve it is obvious that the weight is lost in four well-defined steps, giving at complete decomposition a total weight loss of 58.37% which is comparable to calculated weight loss of 58.11% corresponding to the expected conversion of the oxalate mixture into Co_3O_4-NiO physical mixture. The first two steps are located between 404K and 497K with a mass loss of 19.63%, which corresponds to the loss of crystallization water for the binary mixture. The third step occurs at about 562K with a mass loss of 12.73% due to the decomposition of anhydrous cobalt oxalate and the last step, corresponding to the decomposition of anhydrous nickel oxalate, is accompanied by a mass loss of 26.01% due to the formation of nickel oxide (NiO).

The mass data for the steps of thermal decomposition of the binary mixture at a heating rate of 10K.min^{-1} and the suggested products are listed in TABLE 1.

3.2. DSC analyses

DSC curves at a heating rate of 10K.min^{-1} of the individual oxalates and of the binary mixture are shown in figure 2. The thermal decomposition of the individual oxalates occurs in two steps. The first step is characterized by an endothermic peaks centered at 481K for $CoC_2O_4.2H_2O$ and at 521K for $NiC_2O_4.2H_2O$. They are attributed to the dehydration process. The corresponding enthalpies of average molecular weight are respectively equal to 98.58kJ.mol^{-1} and 97.81kJ.mol^{-1}. The second step, attributed to the oxidative decomposition of the anhydrous oxalates, is characterized by an exothermic peaks centered at 563K for CoC_2O_4 and at 631K for NiC_2O_4. The corresponding enthalpies of average molecular weight are respectively equal to 222.15kJ.mol^{-1} and 167.27kJ.mol^{-1}.

The thermal decomposition of the binary mixture has two endothermic and two exothermic peaks corresponding respectively to the dehydration of the hydrated oxalates and the decomposition of the corresponding anhydrous oxalates. The temperatures of the DSC peaks are well in accordance with that of the DTG peaks, so results of TG-DTG and DSC methods are credible.

The data for the peaks of thermal decomposition of the binary mixture at a heating rate of 10K.min^{-1} in air is in TABLE 2.

3.3. X-ray diffraction analysis

The characteristic parts of X-ray powder diffraction patterns of the parent mixture and its calcined mixtures

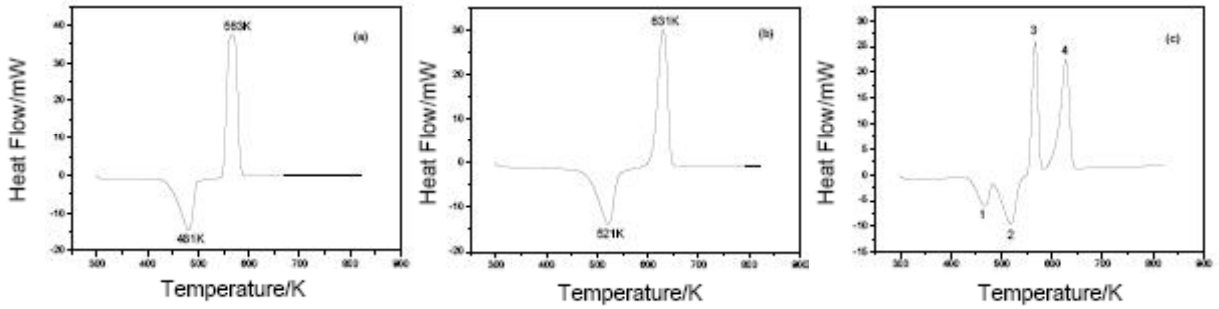

Figure 2: DSC curves of $CoC_2O_4.2H_2O$ (a), $NiC_2O_4.2H_2O$ (b) and the binary mixture (c)

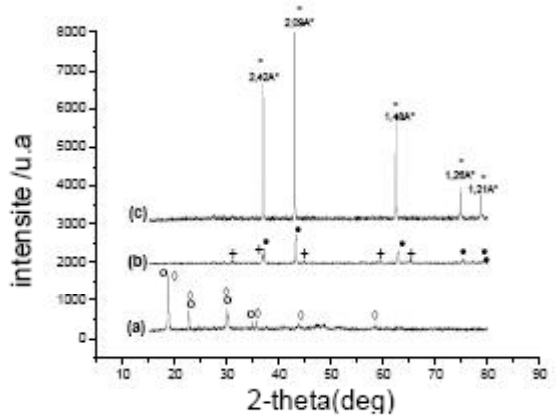

Figure 3 : Characteristic parts of XRD patterns of $CoC_2O_4 \cdot 2H_2O$–$NiC_2O_4 \cdot 2H_2O$ (1:2 mole ratio) mixture calcined at different temperatures: (a) parent mixture; (b) mixture calcined at 873K and (c) mixture calcined at 1273K. Phases: (o) $CoC_2O_4 \cdot 2H_2O$; (◊) $NiC_2O_4 \cdot 2H_2O$; (+) Co_3O_4; (•) NiO; (*) $CoNi_2O_3$

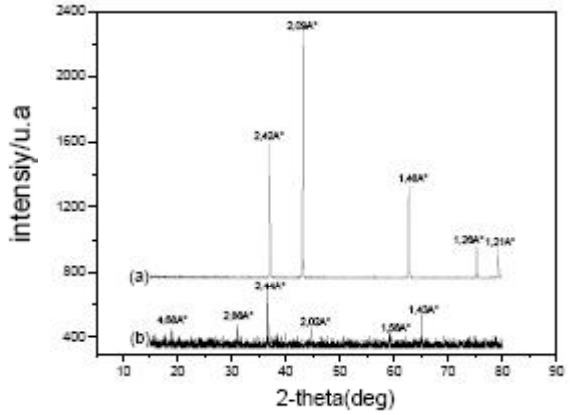

Figure 4: Characteristic parts of XRD patterns of (a) $NiC_2O_4 \cdot 2H_2O$ and (b) $CoC_2O_4 \cdot 2H_2O$ calcined at 1273K

at 873K and 1273K are demonstrated in figure 3. The parent mixture (figure 3a) gave XRD pattern resembles with those reported in the JCPDS data cards of $CoC_2O_4.2H_2O$ (N°25-0250) and $NiC_2O_4.2H_2O$ (N°14-0742).

The XRD pattern of the mixture calcined at 873K (figure 3b) gave the characteristic lines of metal oxide mixture, NiO-Co_3O_4 (JCPDS N°09-0418 and JCPDS N°43-1003 respectively).

TABLE 2: The data for the DSC peaks of thermal decomposition of the binary mixture at a heating rate of 10K.min^{-1} in air

DSC peak	T/K	ΔH (kJ.mol^{-1})
1	468	84.64
2	519	177.81
3	569	238.57
4	629	324.27

For the mixture calcined at 1273K (figure 3c), the peaks relative to Co_3O_4 disappear completely and the intensities of the rest of the XRD lines increase, without changing their positions, which was accompanied by a change in the colour of the mixture compared with that obtained at 873K. These can be attributed to the grain growth and the formation of a well-crystallized solid solution.

To confirm that the new phase obtained at 1273K is a solid solution and not a physical mixture of oxides we have shown in figure 4 the XRD patterns of the individual oxalates calcined at 1273K. In fact, figure 4(a) shows that NiO (JCPDS N° 09-0418) is the final product however, figure 4(b) shows that Co_3O_4 (JCPDS N° 43-1003) is the final product. So if the obtained oxide after calcination of the binary mixture at 1273K was not a solid solution, one would expect to observe XRD lines of Co_3O_4 in figure 3c which was not the case. It is now possible to conclude that at 1273K, the two oxides Co_3O_4 and NiO have yet reacted together to form a well crystallised solid solution of $CoNi_2O_3$.

3.4. FT-IR spectroscopy

Figure 5 shows the FT-IR spectra of different calcined mixtures. The parent mixture gives a spectrum (figure 5a) characteristic for the presence of hydrated metal oxalates. The broad band at 3401 cm^{-1} is assigned

Full Paper

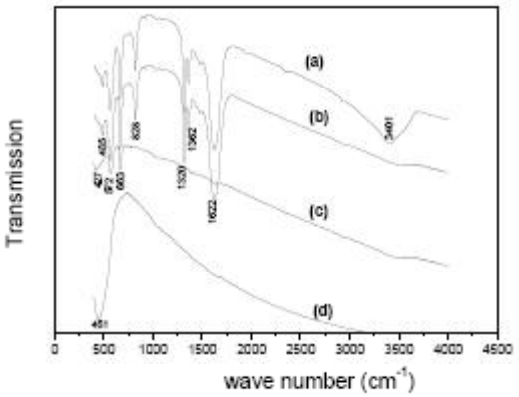

Figure 5: FT-IR spectra of $CoC_2O_4 \cdot 2H_2O$–$NiC_2O_4 \cdot 2H_2O$ (1:2 mole ratio) mixture calcined at different temperatures: (a) parent mixture; (b) mixture calcined at 513K; (c) mixture calcined at 873K; (d) mixture calcined at 1273K

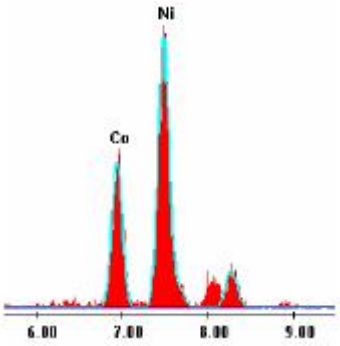

Figure 6: Evidence of Co and Ni in a sample of $CoNi_2O_3$ by EDAX

to the water of hydration. The band at 1622 cm^{-1} is assigned to asymmetric ν(C=O) and the closely spaced bands at 1362 and 1320 cm^{-1} are assigned to symmetric ν(C–O). They indicate the presence of bridging oxalates, with all four oxygen atoms coordinated to the metal atoms[19].

The asymmetric δ(O-C-O) band appeared at 828 cm^{-1}, while the band at 485 cm^{-1} is assigned to ν(M-O) and symmetric δ(C-C-O). The sample calcined at 873K (figure 5c) shows the disappearance of the bands at 3401, 1622, 1362, 1320 and 828 cm^{-1} which suggests the decomposition of all the oxalate content and the formation of the metal oxides. The observed shift to higher frequency is attributed again to the presence of Co_3O_4. The absorption band at 451cm^{-1} which appeared in the spectrum of the mixture calcined at 1273K (figure 5d) is characteristic for $CoNi_2O_3$ solid solution.

3.5.TEM analysis

TABLE 3: Results of compositional analysis

Element	Weight %	Atomic %
Co	33.4	33.3
Ni	66.6	66.7
Total	100	100

The X-ray emission (EDAX) analysis (figure 6) shows that only cobalt and nickel elements are present and that they are found in stoichiometric proportion (TABLE 3).

3.6. Kinetic study by controlled rate thermal analysis

It is widely accepted that conventional thermo gravimetry which subjects samples to a linear heating rate can have a major influence on the information content of the TG curve and on the properties of the heat treated products. This can be a source of irreproducibility and highlights the importance that Constant transformation Rate Thermal Analysis (CRTA) can have[20,21]. CRTA permits a constant reaction rate slow enough to minimise the temperature and pressure gradients within the reacting sample and thus results in a more reproducible experiment[22].

3.6.1. Theory

For experiments carried out in ''isokinetic'' conditions, we can state:

$$\frac{d\alpha}{dt} = C \qquad (1)$$

with

$$\alpha = \frac{\Delta m}{\Delta m_{\infty}} \qquad (2)$$

where Δm is the sample mass loss at time ''t'' and Δm ∞ the final mass loss at time ''t_F''; the rate of reaction, C, is simply measured by the reverse of time needed for the reaction to be completed. Because of the constant rate of evacuation of vapor, the mass losses are directly proportional to the time elapsed, hence, a simple expression of the degree of reaction (or of advancement) α can be obtained:

$$\alpha = \frac{t - t_I}{t_F - t_I} \qquad (3)$$

where t_I is the time of the starting time of the CRTA experiment.

The recording of the sample temperature versus time is then comparable to a TG recording delivering the mass loss versus temperature.

The rate equation for the isokinetic thermal decomposition of solids is often written in the form:

$$\frac{d\alpha}{dt} = Af(\alpha)\exp\left[\frac{-E_a}{RT}\right] \qquad (4)$$

or still

$$T = \frac{Ea}{R\left\{\ln f(\alpha) - \ln\left(\frac{C}{Aa}\right)\right\}} \quad (5)$$

where Ea is the activation energy, Aa is the pre-exponential factor and f(α) the conversion function.

The latter equation, is therefore, suited for describing the degree of reaction versus temperature provided the experiment is carried out isokinetically and provided the reaction studied is characterized by one function f(α), one Arrhenius activation energy Ea and one pre-exponential factor "Aa".

3.6.2.Data processing

3.6.2.1. Thermal decomposition pathway in CRTA conditions

The CRTA curve of the binary mixture (1:2 mol ratio) of oxalates obtained under residual partial vapor pressure of 10^{-3}hPa is shown in figure 7. The temperature curve shows the sample temperature variation with time, controlled so as to keep constant the pressure above the sample. The variation in slope of the temperature curve allows the delimitation of four decomposition steps occurring respectively between 344-367K (A-B), 367-537K (B-C), 537-564K (C-D) and 564-623K (D-E). The length ratio of steps (AB), (BC), (CD) and (DE) is 1/2/2/1 respectively.

According to this result, the two first decomposition steps (AB) and (BC) correspond to the complete dehydration of $CoC_2O_4 \cdot 2H_2O$ and $NiC_2O_4 \cdot 2H_2O$ respectively, whereas steps (CD) and (DE) correspond to the decomposition of the anhydrous Nickel oxalate and cobalt oxalate respectively.

The percentage of mass loss at 623K is found to be 100 $\Delta m/m_0$=68.40%; this is comparable to the theoretical mass loss (67.83%) corresponding to the following steps:

Step (AB): $CoC_2O_4 \cdot 2H_2O(s) \rightarrow CoC_2O_4(s) + 2H_2O(g)$

Step (BC) : $NiC_2O_4 \cdot 2H_2O(s) \rightarrow NiC_2O_4(s) + 2H_2O(g)$

Step (CD) : $NiC_2O_4(s) \rightarrow Ni(s) + 2CO_2(g)$

Step (DE) : $CoC_2O_4(s) \rightarrow Co(s) + 2CO_2(g)$

Thus, the atmosphere surrounding the sample along steps (AB) and (BC) is formed only by the water vapor generated by the sample itself whereas along steps (CD) and (DE) the generated vapor is the carbon dioxide.

Under these conditions, it is possible to consider that dehydration of oxalates occurs at $P_{H20}=10^{-3}$hPa and at constant rate $C=3.93\times10^{-6}s^{-1}$ and that the decomposition of the anhydrous oxalates occurs at $P_{CO_2}=10^{-3}$hPa and at constant rate $C=4.22\times10^{-6}s^{-1}$.

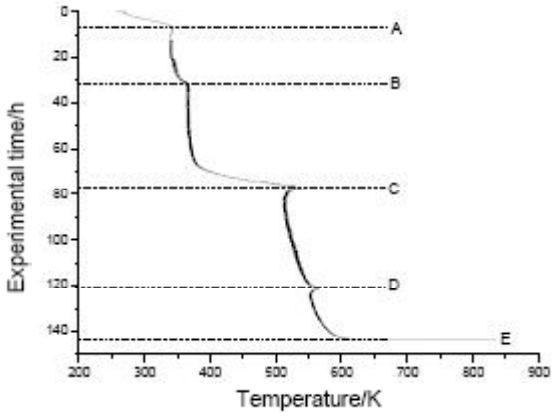

Figure 7: CRTA curve of $CoC_2O_4.2H_2O$-$NiC_2O_4.2H_2O$ (1:2 mole ratio) binary mixture at 10^{-3} hPa partial vapor pressure

3.6.2.2. Measurement of activation energy

The activation energy (Ea) was measured using two CRTA curves obtained under identical conditions of sample mass and residual partial pressure and at two different rates C_1 and C_2 [23].

For a single value of α during an elementary process, without any presumption of the reaction mechanism an expression of the activation energy Ea, at a given value of α, can be obtained from the following equation :

$$Ea = \frac{R \times T_1 \times T_2}{T_2 - T_1} \ln\left[\frac{C_2}{C_1}\right] \quad (6)$$

where T1 and T2 are the temperatures corresponding to the rates C_1 and C_2.

In figure 8 are shown the variations of measured activation energies along the four steps of decomposition carried out at 10^{-3}hPa partial pressure.

The strength of binding of water molecules in the crystal lattice is different and, hence, results in different dehydration temperatures and kinetic parameters. The activation energy for the losing of crystal water lie in the range 60-80 kJ mol^{-1}, while the value for co-ordinately bounded one are within the range 130-160 kJ mol^{-1} [24]. The activation energies found here for the dehydration reactions (figures 8(a and b)) suggest that the water molecules are co-ordinately linked water.

For the oxalates of bivalent metals[25] which produce the metal, the decomposition temperature represents the temperature at which the M-O link is ruptured and

Full Paper

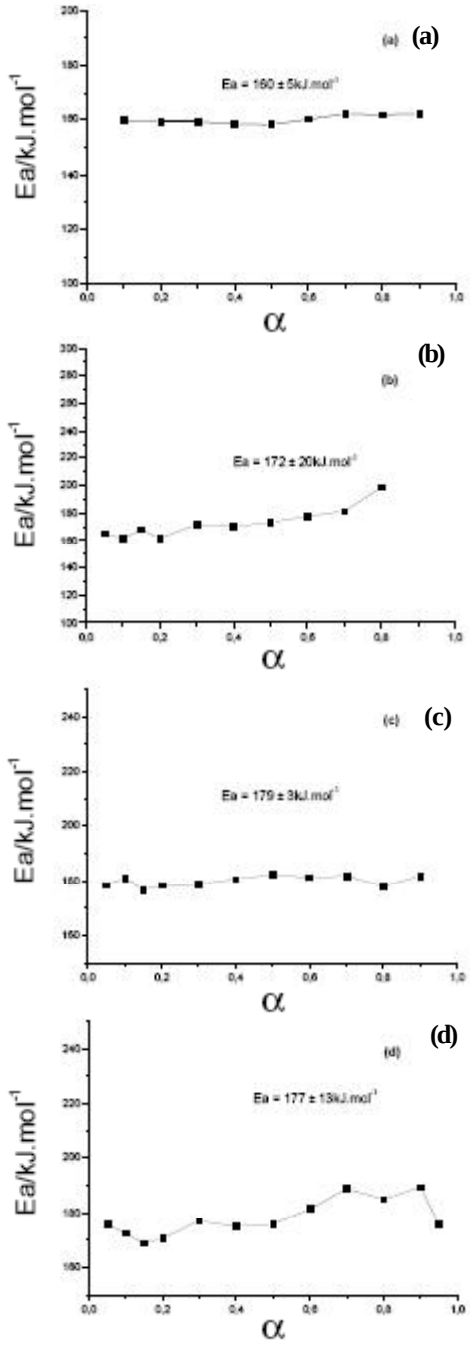

Figure 8. Activation energies measured along the four steps of decomposition at 10^{-3} hPa residual partial pressure. (a) step AB; (b) step BC; (c) step (CD) and (d) step (DE)

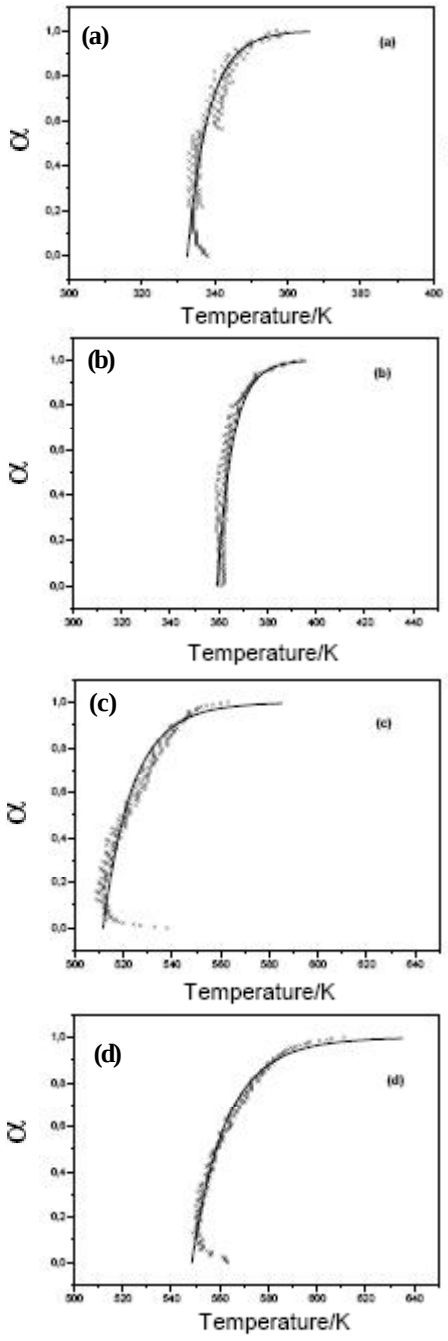

Figure 9: Comparison between experimental CRTA curves (×××) with theoretical curve for F1 model (-)

will depend critically on the size and charge of metal ion. Here the two metals have the same charge and size which can explain the comparable activation energies observed for the decomposition of NiC_2O_4(179kJ. mol^{-1}) and CoC_2O_4 (177kJ.mol^{-1}).

3.6.2.3. Estimation of the conversion function f(α)

The procedure which will be followed here consists to compare theoretical CRTA curve in the case of the nine functions listed by Sharp[26] with the experimental ones. The theoretical CRTA curves are build from the relation ship Eq.5 where Ea is the experimentally measured activation energy and where the mean value of Aa is calculated at α=0,45[27], by means of the selected f(α) function.

In figure 9 are compared the experimental CRTA curves of each step of decomposition with the calculated

CRTA curve corresponding to F1 model. It is clear that F1 model ($f(\alpha)=1-\alpha$) best fits the experimental CRTA curves. This model is known as the first-order model and has been observed in solid-state reactions where the crystallite dimensions are small, such as for fine powders. A single nucleus is generated on each crystallite, and continued growth due to reaction is contained within each individual crystallite. However, if one observes the shape of the experimental CRTA curves (figure 7) we can notice that in order to keep constant all at once pressure above the sample and rate of decomposition, it is necessary that sample tempera ture increases then decreases which is typical of a nucleation process. Then the temperature of the sample has to be continuously increased to maintain constant the pressure indicating a change in the mechanism which corresponds to an instantaneous nucleation model (F1).

4. CONCLUSION

The thermal decomposition of the binary oxalates mixture $CoC_2O_4.2H_2O$-$NiC_2O_4.2H_2O$ (1:2 mole ratio) have been investigated in air using TG-DTG, differential scanning calorimetry (DSC), XRD and FT-IR techniques. The decomposition proceeded through four well-defined steps while TG curves closely corresponded to the theoretical mass loss. The result of XRD showed that the final product formed after calcination of the binary mixture at 1273K is a well-crystallized solid solution $CoNi_2O_3$.

The kinetic of thermal decomposition of the binary mixture was studied using CRTA technique at low residual vapour pressure of 10^{-3}hPa. The activation energy for each step of decomposition was measured experimentally by means of two CRTA curves. The activation energies corresponding to the dehydration of $CoC_2O_4.2H_2O$ and $NiC_2O_4.2H_2O$ at $P_{H_2O}=10^{-3}$ hPa were found equal to 160kJ.mol^{-1} and 172kJ.mol^{-1} respectively whereas those corresponding to the decom positions of NiC_2O_4 and CoC_2O_4 at $P_{CO_2}=10^{-3}$hPa were found equal to 179 kJ.mol^{-1} and 177 kJ.mol^{-1} respectively. The possible conversion function for the dehydration and decomposition of both oxalates kept to the conversion function of "instantaneous nucleation" F1.

5. REFERENCES

[1] F.Medina, P.Salagre, J.L.G.Fierro, J.E.Sueiras; J. Catal., **142**, 392 **(1993)**.

[2] F.Medina, P.Salagre, J.E.Sueiras; J.Chem.Soc., Faraday Trans, **90**, 1455 **(1994)**.

[3] Y.Cesteros, R.Fernandez, J.Estelle, P.Salagre, F. Medina, J.E.Sueiras, J.L.G.Fierro; J.Appl.Catal. A.Gen, **152**, 249 **(1997)**.

[4] Y.Cesteros, P.Salagre, F.Medina, J.E.Sueiras; Appl. Catal.B.Environ., **22**, 135 **(1999)**.

[5] A.Morato, C.Alonso, F.Medina, P.Salagre, J.E. Sueiras, R.Terrado, A.Giralt; J.Appl.Catal.B, Environ., **23**, 175 **(1999)**.

[6] M.M.M.Abd.El-Wahab, R.M.Mahfouz; Thermo chim.Acta, **387**, 63 **(2002)**.

[7] P.Poizot, S.Laruelle, S.Grugeon, L.Dupont, J.M. Tarason; Nature, **407**, 496 **(2000)**.

[8] A.Venkataraman, N.V.Sastry, Arabinda Ray; J.Phys.Chem.Solids, **53**, 681 **(1992)**.

[9] M.A.Gabal, A.A.El-Bellihi, S.S.Ata-Allah; Materials Chemistry and Physics, **81**, 84 **(2003)**.

[10] M.Avrami; J.Chem.Phys., **7**, 1103 **(1939)**.

[11] M.Avrami; J.Chem.Phys., **8**, 212 **(1940)**.

[12] M.Avrami; J.Chem.Phys., **9**, 177 **(1941)**.

[13] B.V.Erofeyev, C.R.Dokl; Acad.Sci.URSS, **52**, 511 **(1946)**.

[14] D.Zhan, C.Cong, K.Diakite, Y.Tao, K.Zhang; Thermochim.Acta, **430**, 101 **(2005)**.

[15] C.S.Carney, C.J.Gump, C.M.Hrenya, A.W.Weimer; Mater.Sci.Eng., **431**, 13 **(2006)**.

[16] Lin Chuanming, Chen Donghua, Tang Wanjun, Peng Yuhua; J.Anal.Appl.Pyrolysis, **75**, 240 **(2006)**.

[17] El-H.M.Diefallah, M.A.Gabal, A.A.El-Bellihi, N.A. Eissa; Thermochim.Acta, **376**, 43 **(2001)**.

[18] J.Rouquerol; J.Thermal.Anal., **5**, 203 **(1973)**.

[19] S.Fronaeus, R.Larsson; Acta Chem.Scand., **14**, 6 **(1960)**.

[20] J.Rouquerol; Thermochim.Acta, **144**, 203 **(1983)**.

[21] O.Toft Sorensen, J.Rouquerol; 'Sample Controlled Thermal Analysis:Origin, Goals, Multiple Forms, Applications and Future', Kluwer Acad., Publishers, Dordrecht, **(2003)**.

[22] J.Rouquerol; J.Therm.Anal.Cal., **72**, 1081 **(2003)**.

[23] Rouquerol, S.Bordere, F.Rouquerol; Thermochim. Acta, **203**, 193 **(1992)**.

[24] El H.M.Diefallah; Thermochim.Acta, **202**, 1 **(1992)**.

[25] El H.M.Diefallah, M.A.Gabal, A.A.El-Bellihi, N.A. Eissa; Thermochim.Acta, **376**, 43 **(2001)**.

[26] J.H.Sharp, G.W.Brindley, B.N.N.Achar; J.Am. Ceram.Soc., **49**, 379 **(1966)**.

[27] K.Nahdi, P.Llewellyn, F.Rouquerol, J.Rouquerol, N.K.Ariguib, M.T.Ayedi, Thermochim.Acta, **390**, 123 **(2002)**.